Preprint
UCRL-JC-137066

Stellar Opacity

F. J. Rogers, C. A. Iglesias

This article was submitted to
American Geophysical Union, Moscone Center
San Francisco, CA
December 13-17, 1999

November 7, 1999

U.S. Department of Energy

Lawrence
Livermore
National
Laboratory

Stellar Opacity

F. J. Rogers and C. A. Iglesias

Lawrence Livermore National Laboratory

Introduction

The monochromatic opacity, κ_ν, quantifies the property of a material to remove energy of frequency ν from a radiation field. A harmonic average of κ_ν, known as the Rosseland mean, κ_R, is frequently used to simplify the calculation of energy transport in stars. The term 'opacity' is commonly understood to refer to κ_R. Opacity plays an important role in stellar modeling because for most stars radiation is the primary mechanism for transporting energy from the nuclear burning region in the core to the surface. Depending on the mass, convection and electron thermal conduction can also be important modes of stellar energy transport. The efficiency of energy transport is related to the temperature gradient, which is directly proportional to the mean radiative opacity in radiation dominated regions. When the radiative opacity is large, convection can become the more efficient energy transport mechanism. Electron conductive opacity, the resistance of matter to thermal conduction, is inversely proportional to electron thermal conductivity. Thermal conduction becomes the dominate mode of energy transport at high density and low temperature.

The removal of energy from a beam of photons as it passes through matter is governed by spectral line absorption (bound-bound), photoelectric absorption (bound-free), inverse Bremsstrahlung (free-free), and photon scattering. Stimulated emission acts as negative opacity by creating photons that add to the beam. Photon scattering is not true photoabsorption; it acts to reduce the photon flux by redirecting photons out of the beam and is not subject to stimulated emission.

The first step in computing the opacity is the determination of the equation of state, followed by the calculation of the various absorption and scattering cross-sections, and finally the integration over frequency to obtain κ_R. Therefore, opacity calculations bring together several distinct disciplines; such as equation of state, atomic physics, spectral line-broadening, as well as plasma collective behavior. These provide ion abundances, energy level values, radiation transition probabilities, spectral line profiles, and structure

factors needed to carry out the calculations. Since atoms from different elements absorb energy of a given frequency at different rates, it is necessary to also know stellar elemental abundances.

Molecules can form in the atmospheres of cool stars. The discussion herein is concerned with stellar interior opacities and does not encompass the molecular regime. The methods for calculating molecular opacities follow a somewhat similar path.

History of opacity calculations

As long ago as 1926 Eddington identified opacity as one of two clouds obscuring stellar model calculations: the source of stellar energy being the other. At that time it was thought that bound-bound absorption was not a significant source of opacity. It was 40 years later that Cox and Stewart included spectral lines in opacity calculations. This led to opacity increases exceeding a factor of three at some temperature-density conditions. These enhanced opacities greatly improved the quality of stellar models. Even so, several properties of stars known to be sensitive to opacity resisted explanation. It was another 20 years before Simon speculated that the most likely explanation was that the heavy element contribution to opacity was still significantly underestimated. Two independent efforts, OPAL and OP, recalculated stellar opacities and found that an improved treatment of atomic data leads to an additional factor of three increase in the opacity under some conditions. The OPAL work was carried out by Iglesias, Rogers, and Wilson. The OP work was carried out by Seaton and a international group of collaborators. These new opacities helped resolve a number of long-standing problems in stellar modeling; particularly in regard to pulsating stars. Direct laboratory verification of the new opacity calculations have only recently started to appear. These show good agreement with the most recent calculations and large differences with standard opacity results used prior to 1985.

Definition of κ_ν

The total extinction from a beam of photons as it passes through matter is given by

$$\kappa_\nu = \kappa_\nu^{abs} + \kappa^s,$$

where

$$\kappa_\nu^{abs} = (1 - e^{-h\nu/kT}) \sum_j x_j \left\{ \kappa_j^{bb} + \kappa_j^{bf} + \kappa_j^{ff} \right\}.$$

is the total photoabsorption, the sum j is over all elements in the mixture, x_j is the elemental number fraction, κ_ν^{bb}, κ_j^{bf}, and κ_j^{ff}, are, respectively, the bound-bound, bound-free, and free-free frequency dependent photoabsorption contributions to opacity, κ^s is the scattering contribution and the factor $\left[1-\exp(-h\nu/kT)\right]$ accounts for stimulated emission. When the density is low enough that the material can be considered to be composed of individual particles, the photon extinction due to a process p is given by,

$$\kappa_\nu^p = \sum_j N_j \sigma_\nu^{pj}$$

where N_j is the number of particles of type j and σ_ν^{pj} is the cross-section for photons of frequency ν.

Mean opacities

The radiation transfer equation describes the transport of energy by photons and is equivalent to the Boltzmann equation in the kinetic theory of particle transport. For steady-state conditions it is given by

$$\frac{dI_\nu(s,\mathbf{n})}{ds} = -\kappa_\nu I_\nu(s,\mathbf{n}) + j_\nu \qquad (1)$$

where $I_\nu(s,\ \mathbf{n})$ is the radiation intensity at frequency ν in the direction $\mathbf{n}$ as a function of distance s, and j_ν is the emissivity.

Stellar interiors are 'collision dominated', so that the material can be considered to be in thermodynamic equilibrium at the local value of temperature and density. Also, due to the small temperature gradient, the radiation intensity is very close to Planckian; i.e. in a state of local thermodynamic equilibrium (LTE). Consequently, Kirchhoff's law,

$$j_\nu = \kappa_\nu B_\nu(T),$$

applies, where

$$B_\nu(T) = (2h\nu^3/c^2)(e^{h\nu/\kappa T}-1)^{-1}$$

is the Planck function. In addition, conditions change slowly over many photon mean-free paths and the radiation flow is nearly isotropic, so that the radiation transfer equation greatly simplifies. In this limit, known as the diffusion approximation, the solution to Eq. (1) as a function of radius, for a non-dispersive medium, integrated over frequency is

$$F(r) = -\frac{4}{3\pi}\frac{1}{\kappa_R}\frac{dB(r,T)}{dr} \tag{2}$$

where $F(r)$ is the total flux, $B(r,T)$ is the integral of B_ν over frequency, and

$$\frac{1}{\kappa_R} = \int_0^\infty d\nu \frac{1}{\kappa_\nu}\frac{dB_\nu}{dT} \Big/ \int_0^\infty d\nu \frac{dB_\nu}{dT}, \tag{3}$$

defines the Rosseland mean opacity. Equation (2) recovers the correct asymptotic solution to the transfer equation and the correct flux transport. The harmonic average in Eq. (3) emphasizes regions of weak absorption, where most of the energy flux is transported. Opacity is normally expressed cm^2g^{-1}. A large value of the opacity indicates strong absorption from a beam of photons, whereas a small value indicates that the beam loses very little energy as it passes through the medium.

Near the surface of a star conditions change very rapidly and the material becomes optically thin. In this limit the assumptions leading to the diffusion approximation break down and a straight arithmetic average of κ_ν^{abs}, known as the Planck mean opacity,

$$k_P = \int_0^\infty d\nu k_\nu^{abs} B_\nu(T) \Big/ \int_0^\infty d\nu B_\nu(T)$$

is more suitable. In contrast to κ_R, strong absorption regions provide the major contributions to the Planck mean opacity. Note also that scattering is not included in the Planck mean.

The mean opacities greatly simplify solutions of the radiation transfer equation, but there are circumstances where it is necessary to use κ_ν directly. An example is radiative driven diffusion in which lowly abundant species are pushed toward the surface due to a net radiation force in the field of the dominate species. This is thought to be the mechanism that causes large over abundances of Mn and Hg in the atmospheres of some late B and A stars.

Equation of state

Equation of state plays an important role in opacity calculations by providing the initial state occupation numbers needed to obtain κ_ν and also by determining the set of final states that exist at particular plasma conditions. This is a statistical mechanics problem that is complicated by the long-ranged Coulomb interaction between the particles. Two types of approaches are used to calculate the equation of state. One is the 'chemical picture' method which is based partly on intuitive reasoning, since it postulates the effect of the plasma on bound states to avoid the divergence of the atomic partition function. Numerous procedures have been proposed, but only one of these receives much current use. It is based on occupation probabilities, w, that separate the statistical weight for a particular state into a part that acts as a localized few body (bound) state and a part $1-w$ that acts as a delocalized (continuum) state. In this approach the bound state energies remain those of an isolated particle, but bound states are effectively destroyed by the action of the surrounding electric microfields when $w \to 0$. This results in a convergent bound state partition function.

The other approach used to calculate the equation of state is known as the 'physical picture' because the starting point is the Coulomb interaction between electrons and nuclei. It is based on an activity expansion of the grand canonical partition function for a plasma. This approach gives directly from theory the plasma effect on bound states and convergent atomic partition functions. (See the heading Equation of State for more details.)

Photoabsorption and Scattering processes

The physical extent of the absorbing atoms and ions in the plasma are generally much less than the wavelength of the radiation, so that only single photon absorption through the electric-dipole interaction is of practical importance in opacity calculations. Electric-quadrapole and magnetic dipole absorption are smaller by several orders of magnitude in the same spectral region. Absorption of two or more photons at a time is also much less likely than single photon absorption and has been shown to be an insignificant source of opacity in stellar plasmas. However, two photons processes are involved in the scattering of radiation. During a scattering event an electron absorbs a photon of frequency ν and immediately re-emits another photon of frequency ν' in an arbitrary direction, effectively removing energy from the beam.

Bound-bound absorption

$$P_i + h\nu \rightarrow P_f .$$

Bound-bound transitions in atoms and ions are possible when the photon frequency is close to $h\nu_{if} = \left(E_f - E_i\right)$, where E_i and E_f are the initial and final state energies. The cross section for this process is given by

$$\sigma_{if}(\nu) = \frac{2\pi^2 e^2}{mc} f\phi_{if}(\nu),$$

where

$$f = \frac{8\pi^2 m\nu_{if}}{3g_i e^2 h}\left|\int_0^\infty \Psi_f^*(\mathbf{r})\mathbf{D}\Psi_i(\mathbf{r})d\mathbf{r}\right|^2 ,$$

is the oscillator strength for the $i \rightarrow f$ transition,

$$\mathbf{D} = e\sum_n \mathbf{r}_n$$

is the dipole moment summed over all the electrons in P_i. m is the electron mass. g_i is the statistical weight, and Ψ_i^* and Ψ_f are the initial and final state wave functions. The total bound-bound cross-section is obtained by summing over all initial and final bound states in the plasma.

The line shape function , $\phi_{if}(\nu)$, includes several processes. Natural broadening is a consequence of the finite lifetime of excited states in the radiation field. It has a normalized Lorentzian profile.

$$\phi(\nu) = 2\pi\Gamma\left[(\nu - \nu_{if})^2 + (\pi\Gamma)^2\right]^{-1},$$

where and Γ is the damping constant. The wings of the Lorentzian fall off as $\Delta\nu^2 = (\nu - \nu_{if})^{-2}$, so that the infra-red wing of the line can be an important source of opacity at very low density. However, the low frequency line profile far from line center is expected to falloff as $\Delta\nu^4$similar to Rayleigh scattering and *ad hoc* methods are sometimes introduced to force this behavior. The thermal velocity distribution of the radiating atoms gives rise to a statistical Doppler shift of radiation frequencies that have a guassian distribution whose wings fall off rapidly compared to $\Delta\nu^2$.

As the density increases, other particles in the vicinity of the radiator increasingly affect the line shape. Electrons and ions are the primary perturbers when the ionization

degree exceeds a few percent, but neutrals can be important at low temperature. There is a large literature associated with the theory of 1 and 2 electron atoms and ions and accurate line shapes are available for these radiators. For hydrogenic ions, where there is degeneracy for levels with the same principal quantum number, the major source of line broadening is due to the linear Stark shift produced by the electric microfield of neighboring ions. In the simplest calculations the ions are assumed to be quasi-static and randomly distributed, leading to the Holtzmark microfield. At high density Coulomb interactions affect the microfield distribution. For practical calculations, electronic collisions with the radiator can be viewed as random fast events compared to the lifetime of the radiator and, since the energy transfers are small, the line shape can be treated by perturbation theory. For helium-like ions the principal quantum number degeneracy is removed for deeply bound states, so that ion perturbations occur through quadratic Stark effect. Electronic contributions are more important in this situation.

The theory of multi-electron atoms and ions, is much less complete, and simple methods are generally used to approximate ϕ_{if}. For radiators with more than two bound electrons, electrons are the major contributor to pressure broadening and the contribution of ions is generally ignored in opacity calculations. The effect of the much faster moving electrons is usually treated in the impact approximation which assumes that only one electron at a time collides with the radiator, instantaneously cutting off its wave train. This approximation also gives a Lorentzian line shape. Assuming the different broadening effects are independent it is possible to convolve the Lorentzian for natural broadening with the Lorentzian for impact broadening to obtain a new Lorentzian whose half-width at half-maximum (HWHM) is just the sum of the HWHM's for natural and pressure broadening. Convolution of this Lorentzian with a Gaussian to account for Doppler broadening then gives a composite shape known as a Voigt profile. Recent line width measurements of Δn =0 transitions in boron and carbon ions indicate that the voigt profiles may provide only a rough approximation. Fortunately, stellar opacity is not very sensitive to moderate changes in line shapes, but this is a source of uncertainty in the calculations.

Bound-free absorption

$$P_i + h\upsilon \rightarrow P_f^+ + e$$

Bound-free transitions are possible when $h\nu$ is greater than the ionization potential, I, of a bound electron. The cross section for this process is

$$\sigma_i^{bf}(\nu) = \frac{4\pi^2}{3g_i c}(I+\varepsilon)\,|\int \Psi_\varepsilon^*(\mathbf{r})\mathbf{D}\Psi_i(\mathbf{r})d\mathbf{r}\,|^2, \qquad (4)$$

where the ejected electron has the energy $\varepsilon = h\nu - I$, and $\Psi_\varepsilon(\mathbf{r})$ is the scattering wave function of the ejected electron. The total cross-section for a given frequency interval is obtained by summing over all initial and final states. Equation. (4) assumes that the photoionization edge is sharp. However, due to the merging of high lying lines just below the continuum, the edge is broadened. Simple procedures, that redistribute the oscillator strength in the vicinity of the edge, are generally introduced to approximate this type of broadening

For complex ions, bound states can overlap in energy with the continuum. If the Hamitonian connects a bound and continuum state, the eigenfunction is mixed introducing resonances into the bound-free continuum , as was first recognized by Fano. This has not been found to have a significant affect on stellar opacity and the autoionizing lines are frequently treated as ordinary broadened lines.

Free-free (inverse Bremsstrahlung) absorption

$$P + e_i + h\upsilon \rightarrow P + e_f$$

For free-free electronic transitions the initial state density is also continuous and its distribution is given by Fermi-statistics. Dipole allowed transitions can only occur in the presence of ions, otherwise energy and momentum cannot be simultaneously conserved. The free-free cross-section can be calculated from the dipole acceleration formulation in the form

$$\sigma^{ff}(\nu) = \frac{e^4}{3\pi\nu^3 m^2 c}\sum_{l_i}\sum_{l_f}\max(l_i,l_f)\delta(l_i - l_f \pm 1)\int_0^\infty \left|\frac{dV}{dr}\right|_{if}^2 p(\varepsilon_i)[1-p(\varepsilon_f)], \qquad (5)$$

where l_i and l_f are the angular momentum of the initial and final states, $\left|dV/dr\right|_{if}$ is the matrix element of the radial derivative of the atomic potential for continuum states i and f, $p(\varepsilon_i)$ is the occupation probability of the initial state, and $1-p(\varepsilon_f)$ is the availability of the final state. Relativistic corrections to σ^{ff} can be significant when $\varepsilon_f > 10$ Kev.

Sampson expressed these corrections for the total scattering cross-section in the form of the multiplicative factor $(n_{ee}/n_e)G(u,T')$, where n_{ee} is the total number of electrons and positrons, n_e is the number of electrons, $u = h\nu/kT$ and $T' = kT/mc^2$. Additional corrections are required if the electrons are degenerate.

Atomic data

Several possible levels of detail in the atomic data needed to calculate the energy levels and oscillator strengths are illustrated in Fig. 1. The example is for transitions that connect two electrons in an sp configuration to a p^2 configuration through a one electron jump. In the simplest case all transitions are assumed to have the same energy. Opacity calculations that carry out a sum over a large number of configurations in this approximation are referred to as detailed configuration accounting (DCA) methods. This was the method used in the earliest bound-bound calculations. However, the DCA approach neglects non-spherical interactions that remove the degeneracy and lead to configuration term structure. In light elements the dominant non-spherical term is the Coulomb interaction between the electrons, which leads to pure LS coupling. In LS coupling the single spectral line of the DCA method in Fig. 1 is split into three distinct lines corresponding to a triplet and two singlet terms. With heavier elements, such as those in the iron group, the interaction between the electron spin and the magnetic field resulting from the electron orbital motion is no longer negligible and require coupling of the LS angular momentum states; known as intermediate coupling. In intermediate coupling the three lines of the LS coupling scheme split into eight lines having no net total spin change, $\Delta S=0$, and 6 intercombination lines having $\Delta S=\pm 1$. For more complicated configurations the increase in the number of spectral lines is more dramatic. For heavy elements this results in a enormous array of spectral lines that can be treated by statistical methods when the density is high enough that these features merge into a quasi-continuum.

The most accurate atomic data is obtained from relativistic self-consistent field methods such as multi-configuration Dirac-Fock (MCDF), but this is very computer intensive when data for millions of transitions is required. The most extensive multi-configuration atomic data tables have been produced by the Opacity Project using the close-coupling method. These calculations are mostly non-relativistic.

Fortunately, the important thing for opacity calculations is the distribution of oscillator strength. The exact locations of lines is only of secondary importance. Consequently single configuration calculations are usually used. Parameterized potentials

have proven to work well for generating the vast amount of data required with accuracy similar to single configuration Hartree-Fock.

[Figure 1]

The effect of elemental composition on stellar properties

Stars are composed mainly of hydrogen and helium whose frequency dependent absorption spectrum is characterized by strong lines separated by regions of weak absorption. Because lowly abundant heavy ions have a more complex absorption spectrum, they contribute disproportionately to κ_R by filling in regions of low absorption in the H-He spectrum.

The total mass of all elements heavier than helium generally comprise less than 2% of the mass of a star. This percentage is known as its 'metallicity'. Even so, lowly abundant elements such as nickel can significantly affect the opacity when the temperature is in the range where the M-shell is partially filled. Because type I stars like the Sun are not old enough that significant burning of elements heavier than helium has occurred, it is normally assumed that these abundances pertain though out the entire star. Consequently for most purposes, it is possible to characterize stellar mixtures with just the three variables X,Y, and Z, where X is the hydrogen mass fraction, Y is the helium mass fraction, and Z is the heavy element mass fraction; i.e. the metallicity. Within this constraint Z can vary, but the abundances of heavy elements relative to each other is fixed. Even without nuclear burning, however, these relative values can vary throughout the star due to diffusion.

Figure 2 compares the monochromatic opacity for a hydrogen-helium mixture with a typical type I stellar composition having Z=0.02. The assumed temperature-density conditions are found in the pulsational driving region of Cepheid variables. The small heavy element admixture dramatically increases the absorption for $u > 3$, corresponding to photon energies above 80 eV; due primarily to transitions originating in the M shells of multiply ionized ions of iron. As a result, even though hydrogen and helium are the most abundant species they are not the main contributors to the opacity at these plasma conditions. They do, nevertheless, play an important role by contributing most of the free electrons that determine the rate of recombination of the heavier elements. These electrons also contribute to electron scattering and free-free absorption.

Figure (3) compares the opacity vs. temperature, for the Sun and a Cepheid variable with a mass 6.5 times solar. Because of their mass difference and location on the Hertzsprung-Russel diagram these stars follow very different temperature-density tracks. The opacity of the solar plasma when heavy elements are left out of the mixture is also

shown. Again heavy elements dominate the opacity throughout most of the stellar interior. For stars of one solar mass or greater core temperatures can exceed 10 million degrees, so that the plasma is highly ionized and even heavy elements like iron may have only a few bound electrons. In this situation the main contributors to opacity are bound-free absorption in heavy elements, free-free absorption from protons and He nuclei, and photon scattering from free electrons. For example, at the solar center the opacity is 40% bound-free, 30% free-free and 30% scattering. In contrast near the solar surface the degree of ionization is very low and since the strongest bound-bound transition energies are large compared to kT, atoms make a very small contribution to opacity. In this case the opacity of H^-, which has a binding energy of only 0.74 eV, is a major contributor to opacity, even though its abundance is generally less than $1.0e^{-7}$. Rayleigh scattering, from H and He is also important near the surface where all atoms are nearly neutral. In the intermediate regions, the opacity is relatively featureless. The maxima near T=40,000 K is in the middle of the H-He ionization zone and is due mainly to bound-bound absorption.

The Cepheid opacity function in Fig. 3 is more complex than the corresponding solar opacity function, displaying two additional local maxima. For the Cepheid the H-He maxima separates into a maxima near T=10,000 K due to H ionization and a maxima near T=40,000 K due to H-He ionization. The third maxima, near T=200,000 K, is due mainly to bound-bound transitions occurring in M-shell iron. For this reason it is known as the 'Z-bump'. The presence of the local maxima near T=40,000 K is what drives the pulsational instability observed for Cepheids, while the Z-bump plays a secondary role by affecting the period ratios between the fundamental mode and its overtones. The solar opacity is much higher at a given temperature, because due to the higher density, the bound states contributing to the bound-bound and bound-free opacity are more highly occupied.

[Figure 2]

[Figure 3]

Plasma environmental effects

The opacity cross-sections discussed above assume that photon extinction processes occur in isolation and ignore the effects due to the surroundings. As the density increases these effects can modify the cross-sections, but are generally small for stellar plasmas. However, for some situations, such as the center of the Sun, relatively small changes in the opacity affect quantities such as the neutrino generation rate through small changes in the estimated temperature. Consequently, there has been theoretical interest in the effect of collective phenomena on opacity. Collective effects due to plasma density oscillations become important when the plasma frequency,

$$\nu_p = \left(\frac{N_e e^2}{\pi m_e} \right),$$

is comparable to the mean photon frequency.

Dispersion

In dispersive media the Planck function in Eq. (3) is modified by the factor n_ν^2 so that the Rosseland mean opacity is given by

$$\frac{1}{\kappa_R} = \int_{\nu_p}^{\infty} d\nu \frac{n_\nu^2}{k_\nu} \frac{dB_\nu}{dT} \Bigg/ \int_0^{\infty} d\nu \frac{dB_\nu}{dT}, \tag{9}$$

where n_ν is the refractive index, which has the approximate form ($\nu > \nu_p$)

$$n_\nu \cong \left[1 - (\nu_p / \nu)^2 \right]^{1/2}.$$

Collective effects also contribute to κ_ν and should be included (see Fig. 4).

Multiple scattering from electrons

When the average photon wavelenght is comparable to the electron-electron correlation length coherent scattering from the electron distribution can occur. When $\nu >> \nu_p$ the Thompson cross-section (Eq. 8) becomes

$$\sigma(\nu) = \frac{3}{8} \int_{-1}^{1} d\mu (1 - \mu)(1 + \mu^2) S_e(q)$$

$$q = \frac{\nu}{2\pi c} \sqrt{2(1 - \mu)}.$$

where $\mu = \cos\vartheta$ and $S_e(q)$ is the electron static structure factor. Correlated scattering from the electron distribution reduces the Thompson Cross-section by 27% at the solar center .

Plasma screening and ion correlations

Plasma screening and ion correlational effects in electron-proton Bremsstrahlung (Eq. 5) can be described through the free-free Gaunt factor. In the (non-relativistic) Born approximation the Gaunt factor can be expressed in the form

$$g_{cor}(\omega) = \frac{\sqrt{3}}{16\pi^3 e^4} \int_0^\infty \frac{dq}{q} \exp\left[-\frac{\hbar^2}{2mkT}\left(\frac{q}{2} - \frac{m\omega}{\hbar q} \right) \right] \left| \frac{q^2 V(q)}{\varepsilon(q,\omega)} \right|^2 S_p(q), \qquad (10)$$

where $\omega = 2\pi\nu$ is the angular frequency, $V(q)$ is the Fourier transform of the Coulomb potential, $S_p(q)$ is the proton static structure factor, and $\varepsilon(q,\omega)$ is the plasma dielectric response function. Similar corrections affect other cross-sections when the density becomes high enough, but are not considered in current calculations. In the low density limit $S_p(q)$ and $\varepsilon(q,\omega) \rightarrow 1$, so that Eq. (10) reduces to the usual Coulomb Gaunt factor.

The effects of plasma dispersion, plasma screening plus ion correlations, and electron degeneracy on electron-proton inverse Bremsstrahlung in the solar center are shown in Fig. 4. Additional dispersion effects appear explicitly in the Rosseland integral Eq. 6. The magnitude of each effect is normalized to the Gaunt factor without these effects included. The corrections are small near $u = 4$ where the largest contributions to the Rosseland integral occur. The reductions in κ_R due to plasma dispersion, screening plus ion correlations, and electron degeneracy, are, respectively, 0.4%, 0.7%, 0.8%. Effects of this size are not generally significant, but they are large enough to be of interest in helioseismic and neutrino flux calculations.

[FIGURE 4]

Acknowledgment

This work was performed under the auspices of the U.S. Department of Energy by the University of California, Lawrence Livermore National Laboratory under Contract No. W-7405-Eng-48.

Bibliography

Adelman S J and Wiese W L eds. 1995 *Astrophysical Applications of Powerful new Databases*, ASP Conf. Ser. Vol **79**

Alexander D R and Ferguson J W 1994 Low-Temperature Rosseland Opacities *Astrophys. J* **437**, 879-891

Iglesias CA, and Rogers F J 1996 Updated OPAL Opacities *Astrophys. J.* **464**, 943

Huebner W F 1986 Atomic and Radiative Process in the Solar Interior. In *Physics of the Sun Vol.* **1**, 33 (Dordrecht: Reidel Publishing Co.) pp 33-74.

Seaton, M 1995, *The Opacity Project*, (Bristol and Philadelphia: Institute of Physics Publishing)

Fig.1. Schematic diagram of possible absorptive transitions between the sp and p^2 configurations in various approximations. Configurational (DCA) transition (*solid arrow*); singlet transition (*short-dashed arrow*); triplet transition (*short-long-dashed arrow*); intercombination transition (*long-dashed arrow*). J is the total angular momentun of the state.

Fig. 2. κ_ν vs. $u = h\nu / kT$ for T=316,000 K and ρ=1x10^{-5} g/cm^3. Results are shown for Z=0 and Z=0.02 with X=0.7 and Y=1-X-Z. The heavy element calculations were carried out in intermediate coupling.

Fig3. Log κ_R vs. log T for the Sun (*solid*) and a Cepheid variable (*dashed*) The assumed heavy element content is Z=0.02. For these stellar tracks, X is around 0.7 for $T < 4$x10^6 K, but is less at higher temperature due to nuclear burning. The upper temperatue limit (1.56x10^{+7} K) corresponds to the solar center. Cepheid core temperatures are about an order of magnitude greater. Also shown is the opacity for the temperatue-density conditions along the solar track assuming Z=0 (*dot-dashed*)

Fig4. Plasma dispersion, screening plus ion correlational, and degeneracy corrections to inverse Bremsstrahlung expressed as ratios $g_{eff}(\nu)/g_o(\nu)$, where g_{eff} is the Gaunt factor including one of these effects and g_o is the Gaunt factor without these effects included. Plasma dispersion (*solid*); screening plus ion correlations (*short-dashed*) , degeneracy (*long-dashed*). The location of the plasma frequency is indicated by u_p.

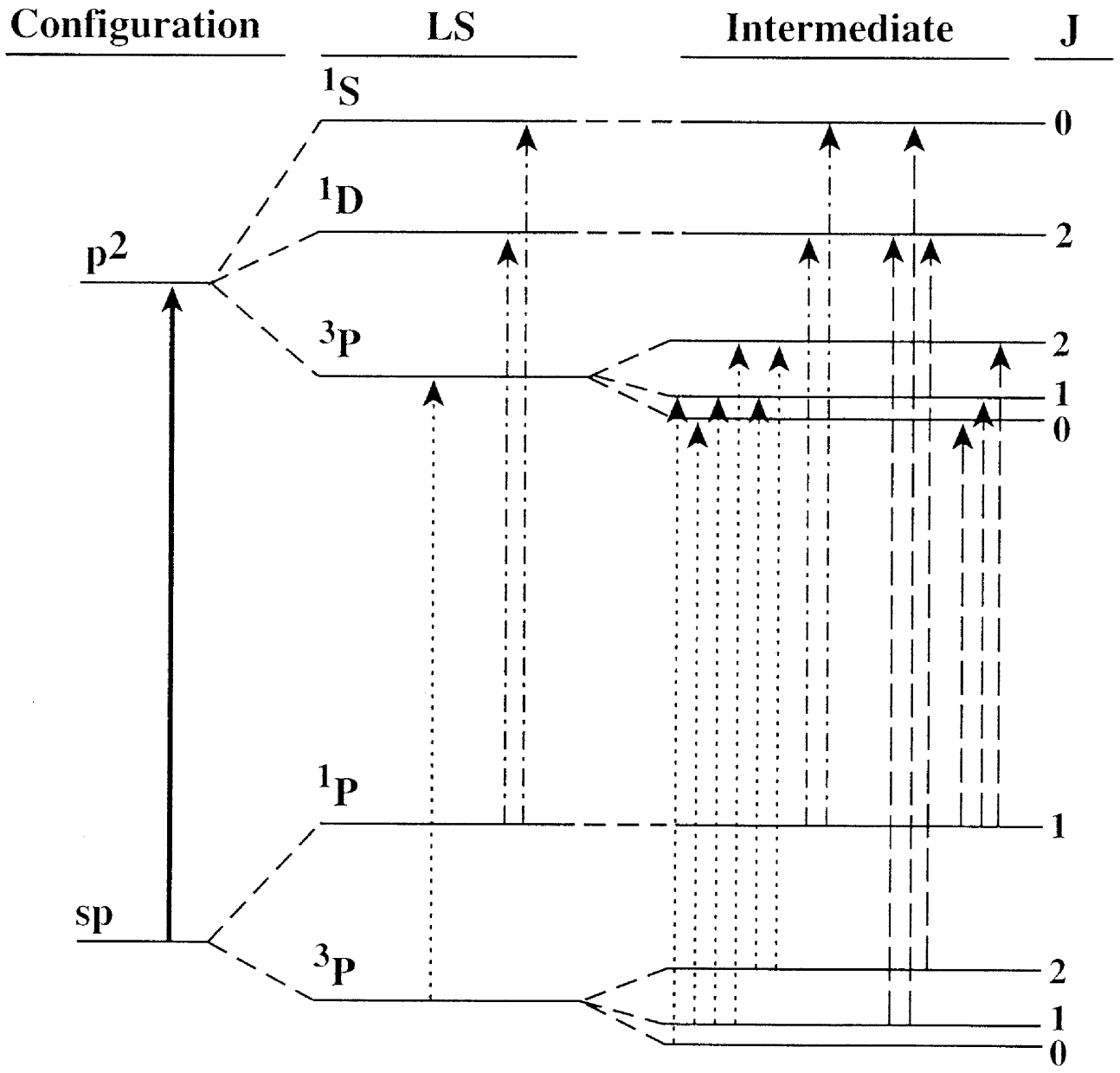
Configuration
LS
Intermediate
J
^1S
^1D
p^2
^3P
^1P
sp
^3P
0
2
2
1
0
1
2
1
0

Figure 1

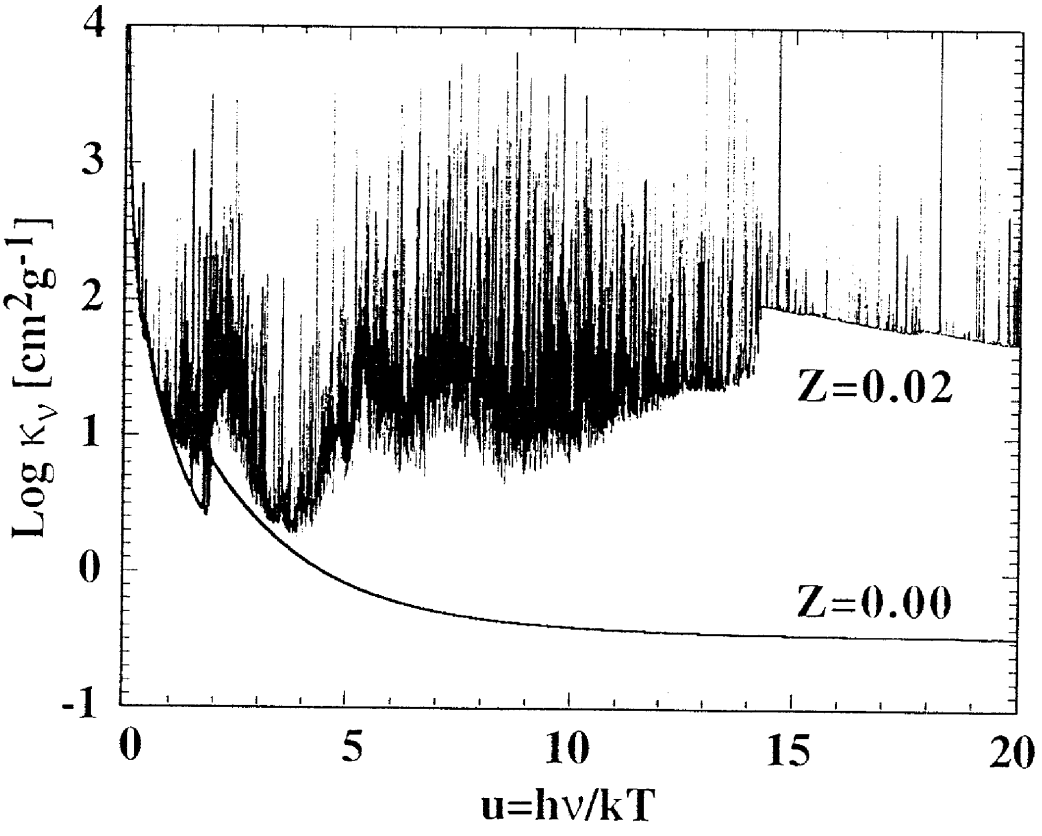

Figure 2

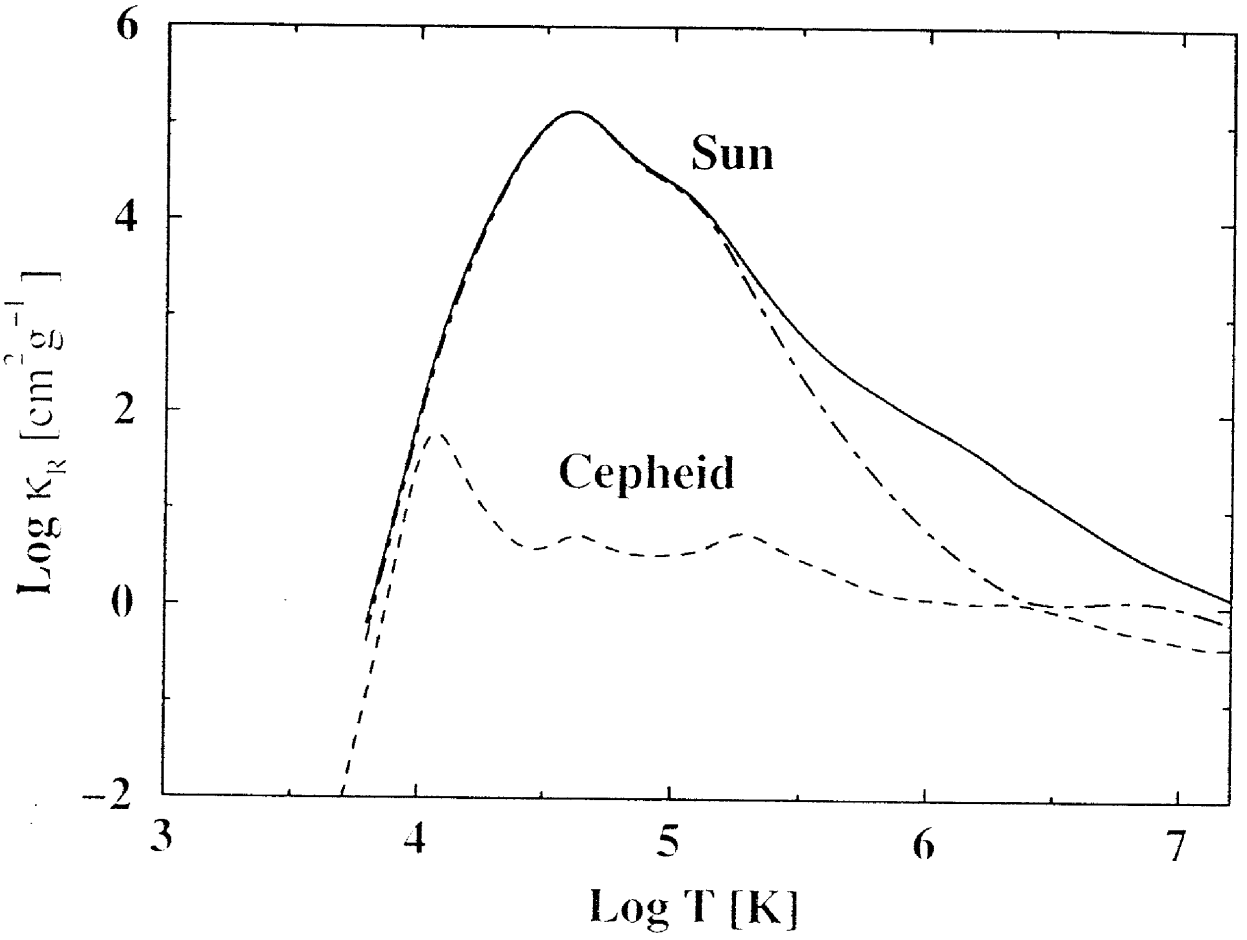

Figure 3

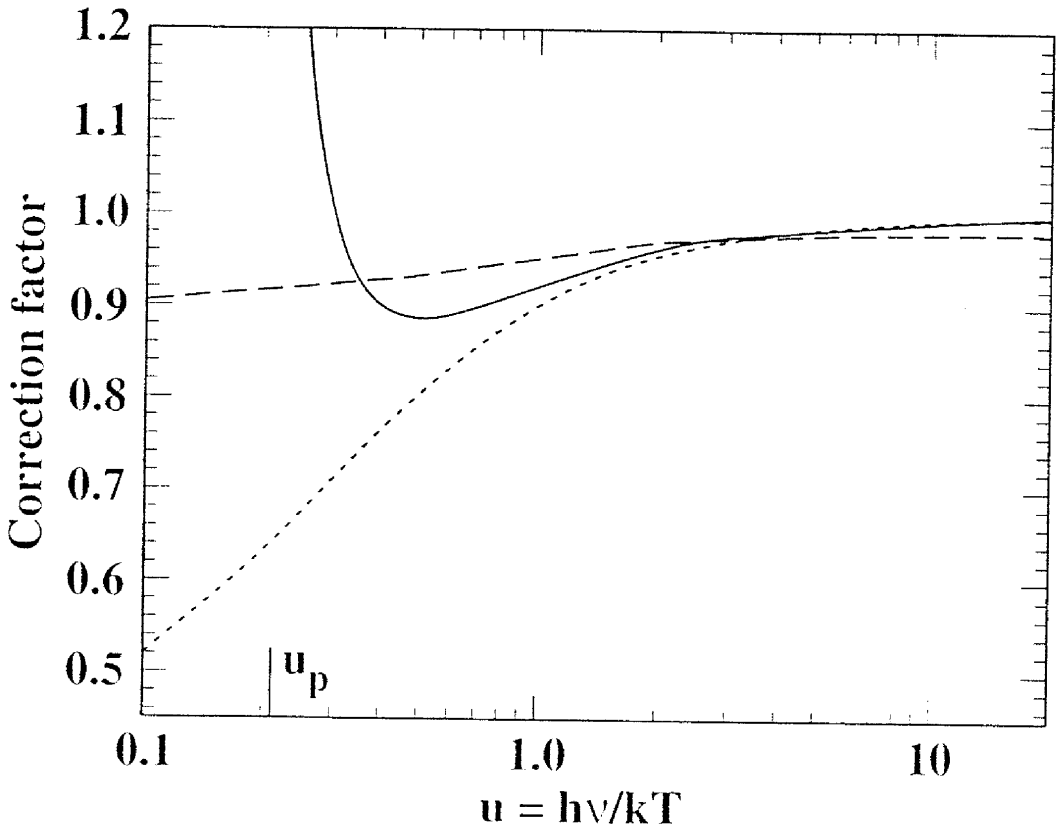

Figure 4

University of California
Lawrence Livermore National Laboratory
Technical Information Department
Livermore, CA 94551